

ARTICLE

Promotion of Ni/MCM-41 Catalyst for Hydrogenation of Naphthalene by co-Impregnation with Polyols

Song-bai Qiu, Yu-jing Weng, Yu-ping Li, Long-long Ma, Qi Zhang, Tie-jun Wang*

Key Laboratory of Renewable Energy, Guangzhou Institute of Energy Conversion, Chinese Academy of Sciences, Guangzhou 510640, China

(Dated: Received on January 11, 2014; Accepted on June 24, 2014)

The activities of nickel supported on MCM-41 catalysts, prepared by co-impregnation with polyols (ethylene glycol, glycerol, xylitol, sorbitol and glucose), were investigated by hydrogenation of naphthalene. Compared with the conventional wetness impregnation, addition of moderate polyols into the metal nitrate aqueous solution could enhance interaction with support surface, resulting in formation of very small NiO particle size (<5 nm), high dispersion of the active phase and significant catalytic activity. Particle size of Ni⁰ decreased from 36.1 nm to below 5 nm; meanwhile the complete hydrogenation of naphthalene was dependent on the Ni⁰ particle size. The hydrogenation activities of the catalysts prepared by co-impregnation with polyols were very high with 100% conversion even at low temperature of 55 °C.

Key words: Ni/MCM-41, co-Impregnation, Naphthalene hydrogenation, Polyols

I. INTRODUCTION

Highly active supported nickel catalysts play key roles in various industrial processes such as olefin hydrogenation, cross-coupling reaction, methanation, steam reforming, hydrocracking, electrochemistry *etc.* [1–4]. Several preparation methods have been developed to obtain highly active catalysts, such as using organic nickel precursor, surface modification, aqueous metal complexes, adjusting pH value of impregnation solution and calcination atmosphere and so on [5–9]. The most used synthesis route involves impregnation of porous support bodies with a solution of the metal precursor followed by evaporation of the solvent. We have developed one simple and novel method to prepare highly active and dispersed metal catalyst by co-impregnation with polyols, which doesn't need too much organic solvent, expensive chelating agents and unusual organic nickel precursors, and the complex preparation process [6]. The most attractive feature of the co-impregnation with ethylene glycol (EG) could be its simplicity in practical execution and potential application in industry [6, 8]. Other polyols, such as glycerol (Gly), xylitol (Xyl), sorbitol (Sor) and glucose (Glu), have similar physical and chemical properties, and play the same role in impregnation as EG. Upon solvent evaporation, additive polyols in the aqueous solution of nickel nitrate was adsorbed onto the support surface for improving the interaction between the metal precursors, which inhibited

redistribution of the active phase over the support bodies during drying, resulting in formation of smaller metal particles [8].

Catalytic hydrogenation of naphthalene was often considered to be the criterion for evaluating the activity of supported nickel catalysts, which is of commercial importance in the fuel upgrading [10]. In order to probe into the influence of additive polyols on the catalytic performance of Ni/MCM-41, naphthalene hydrogenation was used for catalytic test.

II. EXPERIMENTS

Nickels supported on MCM-41 catalysts with 20.0wt%Ni were synthesized via conventional wetness impregnation and co-impregnation [6]. MCM-41 was used as a catalytic support in all catalyst preparations (Tianjin Nankai catalyst company, 100–200 mesh, specific surface area of 1096 m²/g, pore volume of 1.11 cm³/g). In a typical procedure, MCM-41 was impregnated with a Ni(NO₃)₂·6H₂O solution containing polyols (ethylene glycol, glycerol, xylitol, sorbitol and glucose). The molar ratio of Ni:polyols was from 1:0 to 1:3, denoted as Ni:polyols=1:*x*. The mixture was then dried in air under stirring at 100 °C until dryness and calcined at 400 °C for 2 h with a heating rate of 2 °C/min.

Hydrogenation of naphthalene was carried out in a 50 mL stainless steel autoclave equipped with a heating system and a magnetic stir bar. Before hydrogenation, the Ni/MCM-41 samples were reduced at 450 °C in flowing 50% H₂/N₂ for 4 h. In a typical run, 3.2 g of the solution of naphthalene in an *n*-heptane (10.0wt%)

* Author to whom correspondence should be addressed. E-mail: wangtj@ms.giec.ac.cn

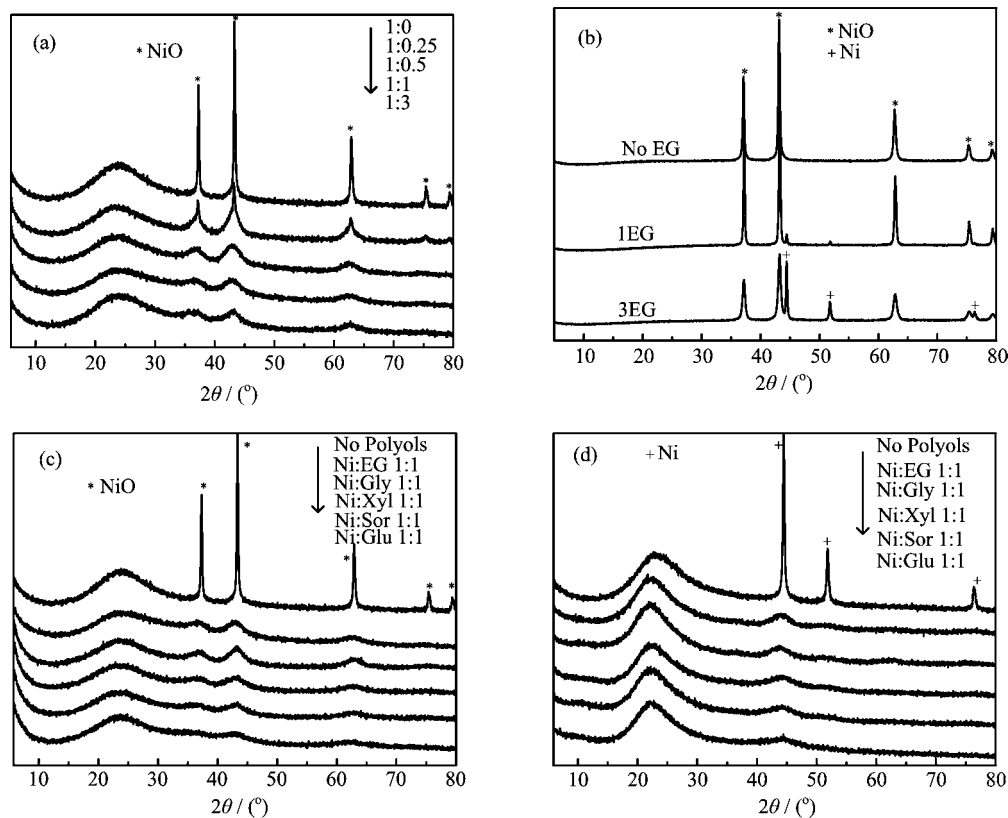


FIG. 1 XRD patterns of various catalysts. (a) Ni/MCM-41 catalysts with different molar ratio of Ni to EG, (b) NiO in the absence of MCM-41 support, (c) Ni/MCM-41 catalysts with different polyols, and (d) the Ni/MCM-41 catalysts after reduction.

and 0.16 g of Ni/MCM-41 catalysts were loaded into the reactor. After 140 min of the reaction, liquid samples were withdrawn from the reactor for subsequent off-line analysis. The components of liquid products were performed by gas chromatograph (Shimadzu GC-2010 with SE-30 capillary column and a flame ionization detector).

The BET specific surface area, average pore diameter and pore volume of catalysts were determined by N_2 isothermal adsorption using QUADRASORB SI analyzer equipped with QuadraWin software system. XRD patterns were recorded by an X'pert Pro Philips diffractometer using $Cu K\alpha$ radiation. The measurement conditions were in the range of $2\theta=5^\circ-80^\circ$, step counting time 10 s, and step size 0.0167° at 298 K. SEM and HRTEM images were determined by a Hitachi S-4800 and a JEOL JEM-2010 microscope, respectively.

III. RESULTS AND DISCUSSION

Figure 1 shows the XRD patterns of the different Ni/MCM-41 catalysts with different ratios of nickel nitrate to polyols. There were three distinct diffraction peaks at $2\theta=37^\circ$, 43° , and 63° , corresponding well with the three most intense peaks of pure cubic NiO. As shown in Fig.1(a), the samples with Ni:EG from

1:0.5 to 1:3 gave weak and broad peaks to NiO, indicating that NiO particles was very small and highly dispersed on the MCM-41 support, while the samples with Ni:EG=1:0 and 1:0.25 showed the strong and sharp NiO peaks, which meant that the NiO particles grew up. The average crystal sizes of NiO decreased gradually from 48.0 nm to below 5 nm with the increasing amount of EG. It was found that the molar ratios of Ni:EG played a vital role in controlling particle sizes and dispersion of NiO on the MCM-41 support.

Figure 1(b) shows the XRD patterns of samples with different ratios of EG to nickel nitrate in the absence of MCM-41 support. When there were no MCM-41 supports, the aqueous solutions of $Ni(NO_3)_2 \cdot 6H_2O$ with EG were directly dried under stirring at $100^\circ C$ for 12 h and then calcined at $400^\circ C$ for 2 h. These peak positions corresponded well with the peaks of cubic NiO. A metal nickel peak associated with the fcc phase for Ni emerges gradually with the increasing amount of EG. During the calcination process, EG decomposition produced a CO/CO_2 -rich atmosphere, which promoted the reduction of the metallic salt [11]. We also prepared the nickel supported catalysts using other polyols with higher carbon chain. The profiles were illustrated in Fig.1(c).

Figure 2 presents the EDS spectrum and their

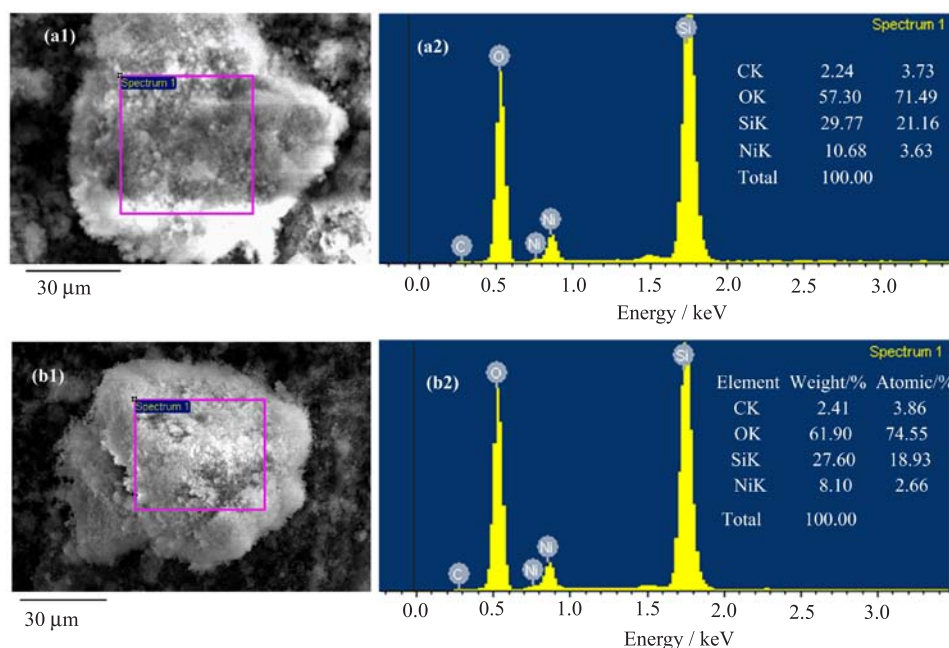


FIG. 2 EDS spectra and their corresponding elemental composition (presented in the inset) of (a) Ni/MCM-41 0EG and (b) Ni/MCM-41 1.0EG catalysts.

corresponding elemental composition of Ni/MCM-41 0EG (the Ni/MCM-41 catalysts without polyols) and Ni/MCM-41 1.0EG (the Ni/MCM-41 catalysts with Ni:polyols=1:1) catalysts. Based on EDS carbon analysis, the surface carbon concentration had a little increase, which revealed the polyols decomposed almost completely during calcining in air. The sample of Ni/MCM-41 0EG also expressed the carbon peak during impregnation without EG, which could be ascribed to carbon pollution or microscanning of carbon belt. Nevertheless, without MCM-41 supports' assistance, the samples did not form very small particles, which indicated strong interaction between supported metal species and MCM-41 surface, leading to the formation of small particle size and uniform dispersion.

The SEM and HRTEM images of Ni/MCM-41 0EG and Ni/MCM-41 1.0EG are also shown in Fig.3. The SEM photographs clearly showed that the samples were irregular shaped and the particle size was micron-sized. Based on the HRTEM images, the Ni/MCM-41 1.0EG catalyst exhibited remarkably smaller particle size. In addition, the NiO nanoparticles were spherical and distributed homogeneously with an average diameter of about 3.5 nm, which was in good agreement with the XRD data, as tabulated in Table I. However, for the Ni/MCM-41 0EG, nickel oxide particle aggregated into even larger clusters on the MCM-41 surface with maldistribution in the range of 20–150 nm. After reduction in flowing 50% H_2/N_2 at 723 K for 4 h, the XRD patterns of NiO entirely disappeared, and the new diffraction peaks of Ni obviously emerged in Fig.1(d). It was observed that the metal Ni^0 kept the approximate crys-

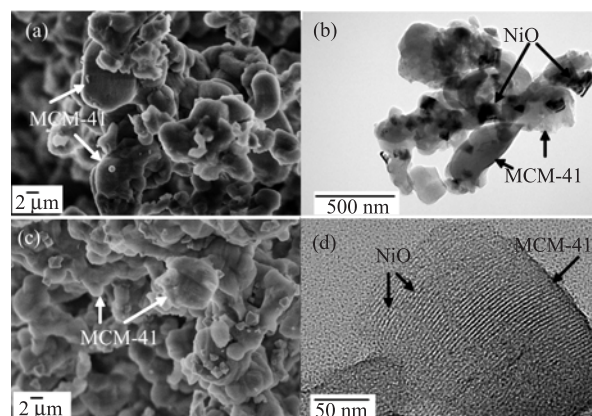


FIG. 3 SEM and HRTEM images of (a, b) Ni/MCM-41 0EG and (c, d) Ni/MCM-41 1.0EG.

tal sizes and dispersion of NiO. According to Scherrer's equation, the nickel crystalline sizes were about 2–3 nm for the Ni/MCM-41 catalysts with Ni:polyols=1:1, and 36.1 nm for the Ni/MCM-41 without polyols addition.

Details of the textural properties derived from isotherms are given in Table I. The data indicated that the BET special surface area and total pore volume decreased significantly after impregnation. The decreased porosity was presumably due to the formation of inaccessible domains in the sample. The impregnation and drying steps did not significantly affect the long-range order of the mesopores. Moreover, the pore diameters for all samples were almost the same as original MCM-41, suggesting that Ni particles were basically limited

TABLE I Textural properties of the catalysts.

Samples	Ni:EG	$S_{\text{BET}}/(\text{m}^2/\text{g})$	Pore volume/ (cm^3/g)	Pore diameter/nm	Mean particle size/nm
MCM41		1103	1.15	2.76	
Ni/MCM41 0EG	1:0	809	0.67	2.75	48.0
Ni/MCM41 1.0EG	1:1.0	785	0.73	2.74	3.2 (3.5 ^a)
Ni/MCM41 1.0Gly	1:1.0	803	0.69	2.74	4.2
Ni/MCM41 1.0Xyl	1:1.0	754	0.65	2.75	2.8
Ni/MCM41 1.0Sor	1:1.0	680	0.52	2.73	2.6
Ni/MCM41 1.0Glu	1:1.0	695	0.54	2.76	2.3

Note: surface areas, pore volumes and diameters of the samples were calculated using standard BET and BJH theory respectively. Particle size was calculated by Scherrer's equation, the Bragg angle of 2θ was 43.3° .

^a Particle size was observed by HRTEM, distributed in the range of 6.2–1.6 nm.

TABLE II Activity of various catalysts under different reaction temperature T_{R} .

Catalyst	$T_{\text{R}}/^\circ\text{C}$	Naphthalene conversion/%	Selectivity/%		
			Tetralin	<i>Trans</i> -decaline	<i>Cis</i> -decaline
Ni/MCM41 0EG	190	100.0	96.8	2.4	0.8
Ni/MCM41 0EG	100	0.4	100.0	0	0
Ni/MCM41 1.0EG	100	100.0	0	37.9	62.1
Ni/MCM41 1.0EG	55	100.0	93.9	2.1	4.0
Ni/MCM41 0.25EG	55	0	Trace	0	0
Ni/MCM41 0.5EG	55	98.9	94.5	1.8	3.7
Ni/MCM41 0.8EG	55	100.0	59.6	17.6	22.8
Ni/MCM41 1.0EG	55	100.0	93.9	2.1	4.0
Ni/MCM41 3.0EG	55	99.0	96.6	1.1	2.3
Ni/MCM41 1.0Gly	100	100.0	0	38.9	61.1
Ni/MCM41 1.0Gly	55	100.0	75.2	9.5	15.3
Ni/MCM41 1.0Xyl	100	100.0	1.0	47.5	52.5
Ni/MCM41 1.0Xyl	55	100.0	8.8	40.0	51.2
Ni/MCM41 1.0Sor	100	100.0	0	43.5	56.5
Ni/MCM41 1.0Sor	55	100.0	36.0	28.9	35.1
Ni/MCM41 1.0Glu	100	100.0	0	45.8	54.2
Ni/MCM41 1.0Glu	55	100.0	0	44.7	55.3

Note: Reaction conditions: 3.2 g of the solution of naphthalene in *n*-heptane (10.0wt%), 0.16 g Ni-MCM41 catalyst, H_2 : 3.0 MPa, 140 min.

on the external surface of the mesoporous support and only some of the MCM-41 was destroyed after metal impregnation [12].

So as to explore the catalytic activity using co-impregnation, the Ni/MCM-41 catalysts were comparatively investigated in the naphthalene hydrogenation. As indicated in Scheme 1, the naphthalene hydrogenation occurred in two sequential steps: the conversion to tetralin first by hydrogenation of one ring, followed by the formation of decalin via hydrogenation of the second ring [13, 14]. The main products were tetralin, *trans*-decalin and *cis*-decalin, and no hydrocracking product was observed. The reaction conditions and product distribution are shown in Table II. Firstly, catalytic performance of Ni/MCM41 catalysts with different molar

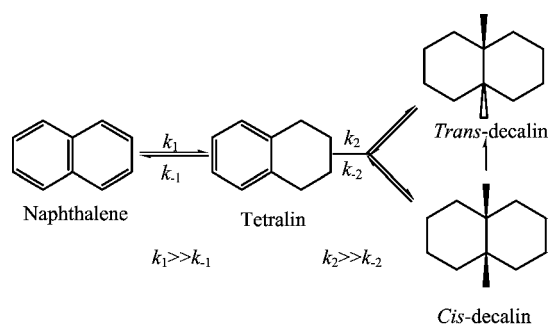
ratios of EG to nickel nitrate was evaluated. When the ratio of EG to nickel nitrate was above 0.5, the particle size calculated from XRD was close, and the catalysts performed the similar activity. Noteworthy, as for the sample with Ni:EG=1:0.25, the catalyst showed little activity for the low temperature hydrogenation of naphthalene. The trend of catalytic activity was in accord with particle size change of Ni supported on MCM-41 with loading of EG, suggesting that small nanoparticles favored low-temperature hydrogenation. On the other hand, if EG was in excess (Ni:EG=1:3), a little decrease of conversion took place, which may be attributed to the increasing carbon residual concentration on the support surface after calcination [15]. Obviously, the nickel supported catalysts prepared using other polyols with

TABLE III The catalytic activity and recycling of Ni-MCM41 1.0EG *vs.* the weight ratio of naphthalene to catalyst.

Weight ratio	Naphthalene conversion/%	Selectivity/%		
		Tetralin	<i>Trans</i> -decalin	<i>Cis</i> -decalin
1:2 ^a (1st)	100.0	93.9	2.1	4.0
1:4	99.5	97.6	0.8	1.6
1:6	99.3	98.5	0.6	0.9
1:20	25.2	99.8	0.1	0.1
1:2 ^a (2nd)	87.2	99.4	0.2	0.4
1:2 ^a (3rd)	56.2	100	0	0

Reaction conditions: reaction temperature of 55 °C. 10.0wt% naphthalene in *n*-heptane solution, 0.16 g Ni-MCM41 1.0EG catalyst, 3.0 MPa H₂, 140 min.

^a Recycling of the catalysts was operated from the first to the third time.



Scheme 1 Reaction pathway of naphthalene hydrogenation.

higher carbon chain possessed of a slight higher activity than the Ni/MCM-41 catalyst using EG. And, tetralin was easily converted into decalin at 55 °C through deep hydrogenating of tetralin. Especially, the catalyst with additive glucose exhibited completely conversion of naphthalene at 55 °C. In comparison with the catalysts prepared by conventional wetness impregnation, the Ni/MCM-41 via co-impregnation with polyols presented super catalytic activity in the naphthalene hydrogenation.

Conversion of naphthalene versus the mass ratio of naphthalene to catalyst and the number of runs was depicted in Table III. The results implied that too many reactants could need more reaction time to be converted to products on the catalyst for some chemical dynamics' reason. The reusability of the catalyst and its activity was investigated by recycling experiments for the hydrogenation of naphthalene performed over the Ni/MCM-41 1.0EG catalyst under the conditions reported. In each cycle the catalyst was washed three times with *n*-heptane to remove residual solvents. A significant drop in conversion of naphthalene was observed after the catalyst was reused twice. It could be concluded that catalyst lost its activity after two runs. For the heterogeneous catalysis, metal species leaching during the reaction is one main problem for recycling [16]. The Ni leaching of active sites on the MCM-41

support might be responsible for the catalytic deactivation, which could presume from the HRTEM images of Ni/MCM-41 1.0EG. This image showed some NiO leaching when the specimen was suspended in ethanol and dispersed ultrasonically.

In a word, the additive polyols during co-impregnation significantly improved the dispersion of supported nickel. Upon solvent evaporation a steep increase in viscosity was apparent, which inhibited redistribution of impregnated solution upon drying of the support bodies, resulting in the formation of small particle size and uniform dispersion [8]. The naphthalene hydrogenation to tetralin was a fast step, and tetralin could be converted to decalin with the increase of reaction temperature on Ni/MCM-41 through deep hydrogenating. Obviously, the big particles of 48 nm NiO were inclined to form tetralin through semihydrogenation due to less activity, while the small particles less than 5 nm had higher activity resulting in further hydrogenation of tetralin, in which apparent reaction rate constants followed a linear relationship with the inverse of the Ni average particle size [13]. Thus, the catalytic activity of Ni/MCM-41 catalysts was strongly enhanced by co-impregnation, apparently related to the ultra small particles and higher dispersion originated from the strong interaction between nickel particles and MCM-41 support [7, 17]. Based on these results, the co-impregnation of polyols into the supports resulted in highly dispersed supported nickel oxide and favored to forming much smaller NiO particle size (<5 nm), contributing to higher catalytic activity in the naphthalene hydrogenation.

IV. CONCLUSION

A simple and practical method for preparing highly active and dispersed supported metal catalysts was developed by co-impregnation with polyols. Upon solvent evaporation, polyols such as glycerol, xylitol, sorbitol and glucose played similar roles in strengthening the interaction between the metal precursors and supports,

which inhibited redistribution of the active phase over the support bodies during drying, resulting in formation of highly dispersed and smaller NiO particles. For the catalysts prepared by co-impregnation with polyols, the NiO particle sizes decreased to below 5 nm from 48 nm, and the hydrogenation activities of naphthalene hydrogenation were very high with 100% conversion even at the low temperature of 55 °C. The catalytic activity of supported catalysts via the simple co-impregnation method was significantly improved, indicating high attraction for potential application in catalysis.

V. ACKNOWLEDGMENTS

This work was supported by the National High-Tech Research and Development 863 Program of China (No.2012AA101806), the National Natural Science Foundation of China (No.21306195 and No.51276183), and the National Key Basic Research Program 973 Project from Ministry of Science and Technology of China (No.2012CB215304).

- [1] A. Stanislaus and B. H. Cooper, *Catal. Rev. Sci. Eng.* **36**, 75 (1994).
- [2] B. W. Hoffer, A. D. V. Langeveld, J. P. Janssens, R. L. C. Bonne, C. M. Lok, and J. A. Moulijn, *J. Catal.* **192**, 432 (2000).
- [3] L. X. Yuan, Y. Q. Chen, C. F. Song, T. Q. Ye, Q. X. Guo, Q. S. Zhu, Y. Torimoto, and Q. X. Li, *Chem. Commun.* **41**, 5215 (2008).
- [4] L. X. Yuan, T. Q. Ye, F. Y. Gong, and Q. X. Li, *Chin. J. Chem. Phys.* **22**, 34 (2009).
- [5] F. Li, X. D. Yi, and W. P. Fang, *Catal. Lett.* **130**, 335 (2009).
- [6] S. B. Qiu, X. Zhang, Q. Y. Liu, T. J. Wang, Q. Zhang, and L. L. Ma, *Catal. Commun.* **42**, 73 (2013).
- [7] J. F. Chen, Y. R. Zhang, L. Tan, and Y. Zhang, *Ind. Eng. Chem. Res.* **50**, 4212 (2011).
- [8] A. J. Dillen, R. M. Terörde, D. J. Lensveld, J. W. Geus, and K. P. Jong, *J. Catal.* **216**, 257 (2003).
- [9] C. H. Bartholomew, R. B. Pannell, and J. L. Butler, *J. Catal.* **65**, 335 (1980).
- [10] S. R. Kirumakki, B. G. Shpeizer, G. V. Sagar, K. V. R. Chary, and A. Clearfield, *J. Catal.* **242**, 319 (2006).
- [11] Y. Wu, Y. M. He, T. H. Wu, T. Chen, W. Z. Weng, and H. L. Wan, *Mater. Lett.* **61**, 3174 (2007).
- [12] B. Xue, H. Li, J. Xu, P. Liu, Y. Zhang, and Y. X. Li, *Catal. Commun.* **29**, 153 (2012).
- [13] R. Nares, R. Jorge, G. A. Aida, and R. Cuevas, *Ind. Eng. Chem. Res.* **48**, 1154 (2009).
- [14] A. Corma, A. Martiniz, and V. Martiniz-soria, *J. Catal.* **169**, 480 (1997).
- [15] D. Valencia and T. Klimova, *Appl. Catal. B* **129**, 137 (2013).
- [16] P. Albers, J. Pietsch, and S. F. Parker, *J. Mol. Catal. A* **173**, 275 (2001).
- [17] Z. P. Qu, W. X. Huang, S. T. Zhou, H. Zheng, X. M. Liu, M. J. Cheng, and X. H. Bao, *J. Catal.* **234**, 33 (2005).